LATTICE 2026

UNIVERSITY OF MARYLAND, COLLEGE PARK

Progress on bottom-baryon decay form factors from lattice QCD

Stefan Meinel

The University of Arizona

Overview: bottom-baryon decay form factors from lattice QCD

Early lattice studies of $\Lambda_b \to \Lambda_c$ (quenched, focused on Isgur-Wise function):

K. C. Bowler *et al.* (UKQCD Collaboration), hep-lat/9709028/PRD 1998 ; S. Gottlieb and S. Tamhankar, hep-lat/0301022/Lattice 2002

Our lattice calculations, using RBC/UKQCD gauge-field configurations, $N_f = 2+1$

Transition	m_Q	a [fm]	m_π [MeV]	Reference
$\Lambda_b \to \Lambda$	∞	0.08, 0.11	230–360	WD, DL, SM, MW, 1212.4827/PRD 2013
$\Lambda_b \to p$	∞	0.08, 0.11	230–360	WD, DL, SM, MW, 1306.0446/PRD 2013
$\Lambda_b \to p$	phys.	0.08, 0.11	230–360	WD, CL, SM, 1503.01421/PRD 2015
$\Lambda_b \to \Lambda_c$	phys.	0.08, 0.11	230–360	WD, CL, SM, 1503.01421/PRD 2015;
				AD, SK, SM, AR, 1702.02243/JHEP 2017
$\Lambda_b \to \Lambda$	phys.	0.08, 0.11	230–360	WD, SM, 1602.01399/PRD 2016
$\Lambda_b \to \Lambda^*(1520)$	phys.	0.08, 0.11	300–430	SM, GR, 2009.09313/PRD 2021; 2107.13140/PRD 2022
$\Lambda_b \to \Lambda_c^*(2595)$	phys.	0.08, 0.11	300–430	SM, GR, 2103.08775/PRD 2021; 2107.13140/PRD 2022
$\Lambda_b \to \Lambda_c^*(2625)$	phys.	0.08, 0.11	300–430	SM, GR, 2103.08775/PRD 2021; 2107.13140/PRD 2022
$\Xi_b \to \Xi$	phys.	0.07, 0.08, 0.11	230–430	CF, SM, 2603.18438/PRD 2026
$\Lambda_b \to p, \Lambda, \Lambda_c$	phys.	0.07, 0.08, 0.11	140–360	SM, in preparation

Charged-current Λ_b decays

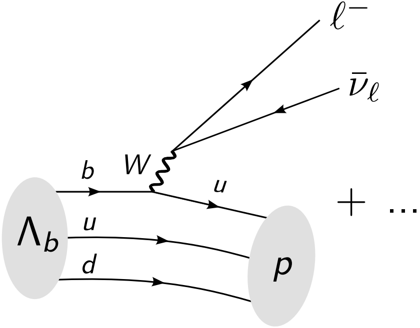

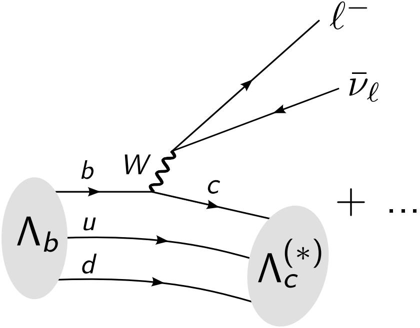

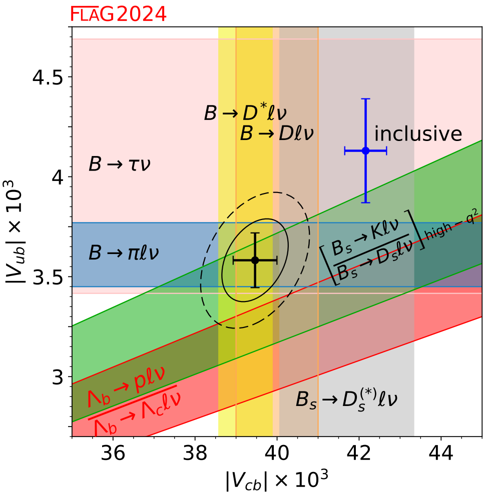

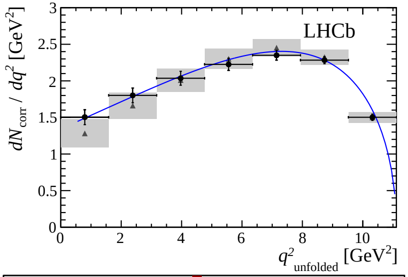

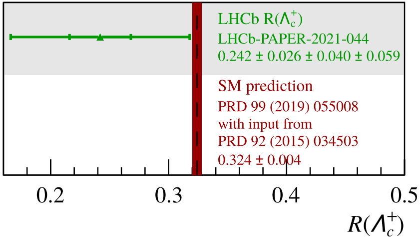

LHCb results: 1504.01568/Nature Phys. 2015; 1709.01920/PRD 2017; 2201.03497/PRL 2022

Rare Λ_b decays

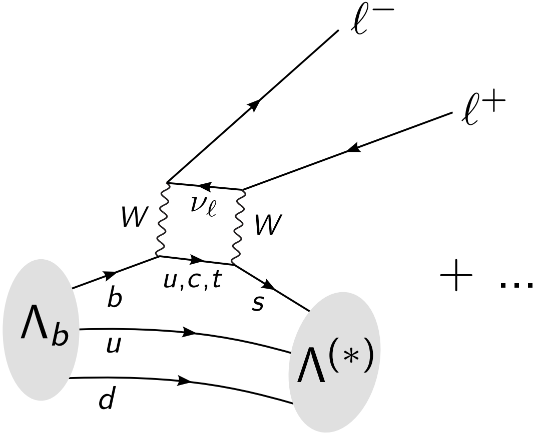

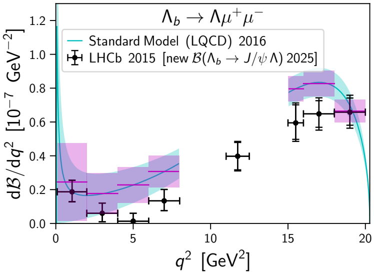

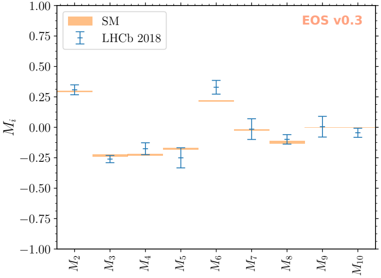

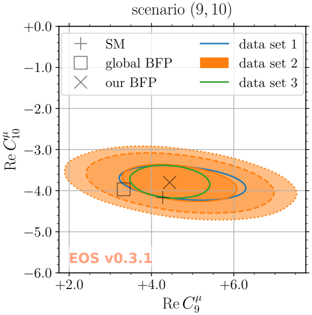

[W. Detmold, S. Meinel, 1602.01399/PRD 2016]

[T. Blake, S. Meinel, D. van Dyk, 1912.05811/PRD 2020]

[LHCb, 1503.07138/JHEP 2015; 2509.12805/JHEP 2026]

[LHCb, 1808.00264/JHEP 2018]

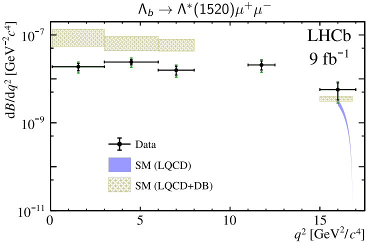

[LQCD: S. Meinel, G. Rendon, 2107.13140/PRD 2022; LHCb: 2302.08262/PRL 2023]

What about rare decays of other b baryons?

LHCb is also analyzing Ξ_b^- decays. Low production fraction but distinctive final states.

- $\Xi_b^- \to \Xi^- \gamma$

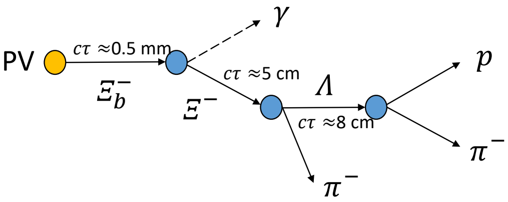

First result: $\mathcal{B}(\Xi_b^- \to \Xi^- \gamma) < 1.3 \times 10^{-4}$ at 95% CL [LHCb, 2108.07678/JHEP 2022]

- $\Xi_b^- \to \Xi^- \mu^+ \mu^-$

Analysis in progress

[Janina Nicolini, https://indico.mitp.uni-mainz.de/event/460/contributions/6038/]

 

$\Xi_b \to \Xi$ form factors from lattice QCD and Standard-Model predictions for $\Xi_b \to \Xi\mu^+\mu^-$ and $\Xi_b \to \Xi\gamma$ decays

Callum Farrell and Stefan Meinel
Department of Physics, University of Arizona, Tucson, AZ 85721, USA
(Dated: March 18, 2026)

We present the first lattice QCD determination of the $\Xi_b \to \Xi$ vector, axial-vector, and tensor form factors, which are relevant for the theory of rare decays including $\Xi_b \to \Xi\ell^+\ell^-$ and $\Xi_b \to \Xi\gamma$. The calculation is performed with 2+1 flavors of domain-wall fermions at three different lattice spacings and pion masses in the range from approximately 430 to 230 MeV. The bottom quark is implemented using an anisotropic clover action. Three-point functions with a wide range of source-sink separations and model averaging are used to extract the ground-state contributions. We fit the dependence of the form factors on the momentum transfer, the pion mass, and the lattice spacing using modified z expansions that account for subthreshold branch cuts, and apply dispersive bounds and asymptotic-behavior constraints to achieve controlled uncertainties in the full semileptonic kinematic region. Using our form factor results, we present Standard-Model predictions for the $\Xi_b^- \to \Xi^-\gamma$ and $\Xi_b^- \to \Xi^-\mu^+\mu^-$ branching fractions and two angular observables.

[2603.18438/PRD 2026]

Local form factors

Current	Form factors
Vector	f_0, f_+, $f_\perp$
Axial vector	g_0, g_+, $g_\perp$
Tensor	h_+, $h_\perp$, $\widetilde{h}_+$, $\widetilde{h}_\perp$

Example:

$$\begin{aligned}\langle \Xi(p',s')|\bar{s}\gamma^\mu\gamma_5 b|\Xi_b(p,s)\rangle \quad &= \quad -\overline{u}_\Xi(p',s')\,\gamma_5\Big[(m_{\Xi_b}+m_\Xi)\frac{q^\mu}{q^2}\,g_0(q^2) \\ &\quad + \frac{m_{\Xi_b}-m_\Xi}{s_-}\left(p^\mu + p'^\mu - (m_{\Xi_b}^2 - m_\Xi^2)\frac{q^\mu}{q^2}\right) g_+(q^2) \\ &\quad + \left(\gamma^\mu + \frac{2m_\Xi}{s_-}p^\mu - \frac{2m_{\Xi_b}}{s_-}p'^\mu\right) g_\perp(q^2)\Big] u_{\Xi_b}(p,s)\end{aligned}$$

where $q = p - p'$ and $s_\pm = (m_{\Xi_b} \pm m_\Xi)^2 - q^2$ [T. Feldmann, M. W. Y. Yip, 1111.1844/PRD 2012]

Lattice actions and ensembles

- Gluons: Iwasaki action
- u, d, s quarks: domain-wall action
- Gauge configurations generated by RBC/UKQCD

Label	$N_s^3 \times N_t$	β	$am_{u,d}^{(\text{sea,val})}$	$am_s^{(\text{sea})}$	$am_s^{(\text{val})}$	a [fm]	$m_\pi^{(\text{sea,val})}$ [MeV]	Samples
C01	$24^3 \times 64$	2.13	0.01	0.04	0.0323	≈ 0.111	≈ 430	283 ex, 2264 sl
C005	$24^3 \times 64$	2.13	0.005	0.04	0.0323	≈ 0.111	≈ 340	311 ex, 2488 sl
F004	$32^3 \times 64$	2.25	0.004	0.03	0.0248	≈ 0.083	≈ 300	251 ex, 2008 sl
F1M	$48^3 \times 96$	2.31	0.002144	0.02144	0.02217	≈ 0.073	≈ 230	113 ex, 1808 sl

Lattice actions and ensembles

- b quarks: anisotropic clover action

$$S_Q = a^4 \sum_x \bar{Q} \left[m_Q + \gamma_0 \nabla_0 - \frac{a}{2} \nabla_0^{(2)} + \nu \sum_{i=1}^{3} \left(\gamma_i \nabla_i - \frac{a}{2} \nabla_i^{(2)} \right) - c_E \frac{a}{2} \sum_{i=1}^{3} \sigma_{0i} F_{0i} - c_B \frac{a}{4} \sum_{i,j=1}^{3} \sigma_{ij} F_{ij} \right] Q$$

with m_Q, ν, $c_E = c_B$ tuned nonperturbatively using B_s energy, "speed of light" $c^2 = M_{\rm rest}/M_{\rm kin}$, and hyperfine splitting. This removes all $(am_Q)^n$ discretization errors in on-shell observables. [Y. Aoki *et al.*, 1206.2554/PRD 2012]

Ensemble	am_Q	ν	$c_{E,B}$	aE_{B_s}	E_{B_s} [GeV]	$c^2_{B_s}$	$aE_{B_s^*} - aE_{B_s}$	$E_{B_s^*} - E_{B_s}$ [MeV]
C005	7.42	2.92	4.86	3.00324(81)	5.360(15)	0.9184(89)	0.02602(52)	46.44(94)
C005	7.471	2.929	4.92	3.00801(81)	5.369(15)	0.9184(89)	0.02616(53)	46.69(95)
C005	7.9	2.929	4.92	3.05463(85)	5.452(15)	0.8895(91)	0.02482(53)	44.29(96)
C005	7.471	2.929	6	2.97872(77)	5.316(15)	0.9399(85)	0.03165(58)	56.5(1.1)
C005	7.471	3.3	4.92	3.03049(75)	5.409(15)	1.0186(89)	0.02665(48)	47.56(86)
C005	7.3258	3.1918	4.9625	3.00695(75)	5.367(15)	1.0013(88)	0.02719(49)	48.52(88)
F004	3.485	1.76	3.06	2.25010(82)	5.363(19)	0.855(12)	0.02053(62)	48.9(1.5)
F004	3.3	1.76	3.06	2.20958(79)	5.266(19)	0.877(12)	0.02148(61)	51.2(1.5)
F004	3.485	1.76	3.7	2.21551(78)	5.280(19)	0.877(12)	0.02468(68)	58.8(1.6)
F004	3.485	2.2	3.06	2.29690(70)	5.474(20)	1.047(12)	0.02126(51)	50.7(1.2)
F004	3.2823	2.0600	2.7960	2.25175(71)	5.366(19)	1.004(12)	0.02046(51)	48.8(1.2)
F1M	2.4538	1.7563	2.6522	1.97455(85)	5.347(20)	0.960(16)	0.01876(79)	50.8(2.2)
F1M	2.55	1.7563	2.6522	2.00012(88)	5.416(20)	0.943(17)	0.01821(81)	49.3(2.2)
F1M	2.4538	2	2.6522	2.00698(75)	5.435(20)	1.089(16)	0.01926(70)	52.2(1.9)
F1M	2.4538	1.7563	3.1	1.94472(81)	5.266(20)	0.983(16)	0.02151(83)	58.3(2.3)
F1M	2.3867	1.8323	2.4262	1.98009(81)	5.362(20)	1.003(16)	0.01799(73)	48.7(2.0)

[S. Meinel, 2309.01821/PoS 2024]

Renormalization and improvement of weak currents

We use the "mostly nonperturbative method" to renormalize the currents,

$$J_\Gamma = \sqrt{Z_V^{qq}\, Z_V^{QQ}}\ \rho_\Gamma \left[\bar{q}\,\Gamma\, Q + \mathcal{O}(a)\right],$$

where

■ = nonperturbative renormalization factors of $\bar{q}\gamma^0 q$ and $\bar{Q}\gamma^0 Q$ determined using charge conservation,
■ = one-loop residual-matching and $O(a)$-improvement coefficients, computed by Christoph Lehner.

[S. Hashimoto *et al.*, hep-ph/9906376/PRD 1999; A. El-Khadra *et al.*, hep-ph/0101023/PRD 2001]

For tensor currents, ρ_Γ and $\mathcal{O}(a)$ terms at tree level only.

Extraction of the form factors from correlation functions

Each form factor f is obtained from the large-t limit (t = Euclidean-time source-sink separation) of a combination of three-point and two-point correlation functions,

$R_f =$ $\sqrt{\quad}$ (kinematic factors) $\times$

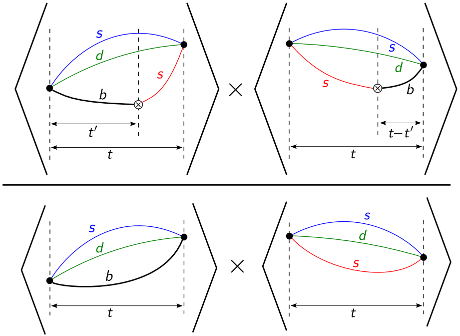

where we are setting $t' = t/2$.

Extraction of the form factors from correlation functions

$R_f(t) \to f$ for large t. We use fits of the form $R_f(t) = f + A\, e^{-\Delta E\, t}$, where f, A, ΔE are fit parameters.

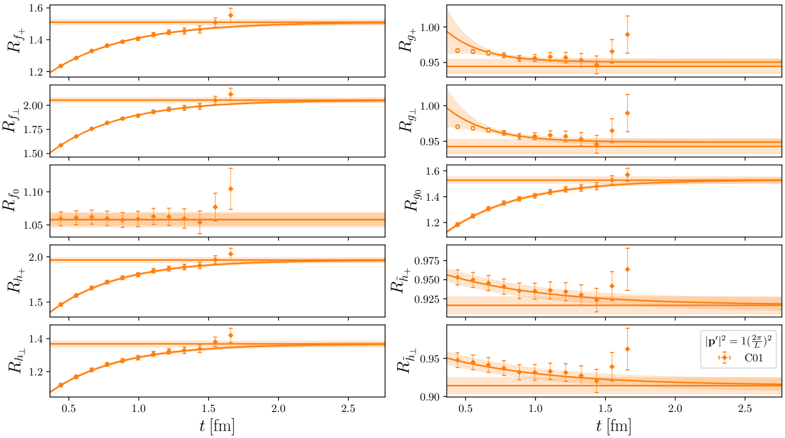

We use the "perfect model" version of the Akaike information criterion to average over fits with different t_{min} [W. Jay and E. Neil, 2008.01069/PRD 2021]. Horizontal bands = AIC averages of f

Extraction of the form factors from correlation functions

$R_f(t) \to f$ for large t. We use fits of the form $R_f(t) = f + A\, e^{-\Delta E\, t}$, where f, A, ΔE are fit parameters.

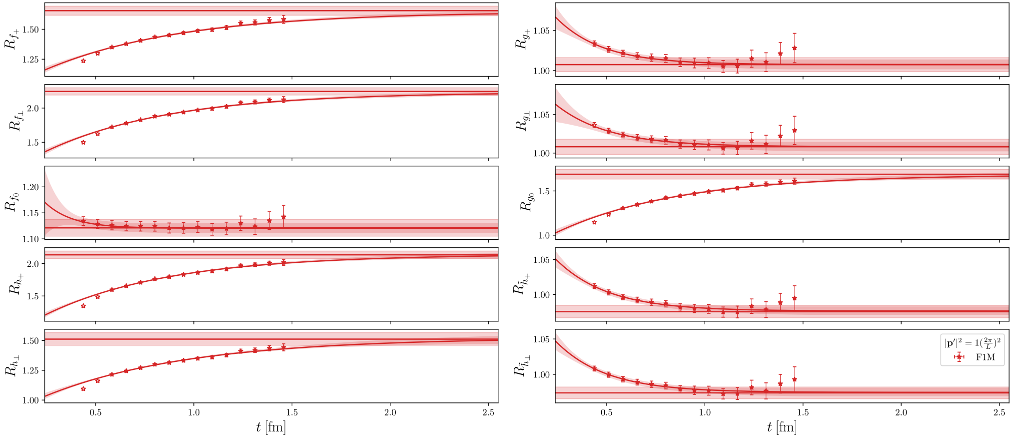

We use the "perfect model" version of the Akaike information criterion to average over fits with different $t_{\min}$ [W. Jay and E. Neil, 2008.01069/PRD 2021]. Horizontal bands = AIC averages of f

Chiral-continuum-kinematic extrapolations

Example:

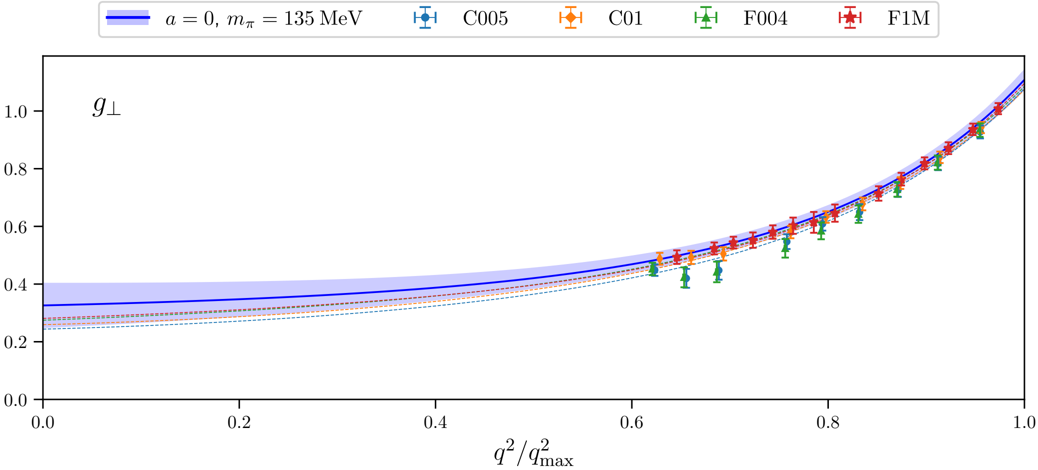

The fit is done using a modified z expansion of order z^8 with a dispersive bound on the coefficients and additional constraints ensuring reasonable asymptotic behavior for $q^2 \to -\infty$.

Dispersive bounds

[T. Blake, S. Meinel, M. Rahimi, D. van Dyk, 2205.06041/PRD 2023]

An example of a dispersive bound is

$$\underbrace{\chi_V^{J=1}(Q^2)\Big|_{\text{OPE}}}_{\text{perturbation theory}} > \int_{t_{\text{th}}}^{\infty} \mathrm{d}t\, \frac{1}{24\pi^2} \frac{\sqrt{\lambda(m_{\Xi_b}^2, m_{\Xi}^2, t)}}{t^2(t-Q^2)^3} s_-(t) \left((m_{\Xi_b} + m_{\Xi})^2 |f_+(t)|^2 + 2t |f_\perp(t)|^2 \right),$$

where $t_{\text{th}} = (m_{\Xi_b} + m_{\Xi})^2$, $\quad \chi_V^{J=1}(Q^2) = \frac{1}{2!} \left(\frac{\mathrm{d}}{\mathrm{d}Q^2} \right)^2 \Pi_V^{J=1}(Q^2)$, $\quad$ and we use $Q^2 = 0$.

NB: 2205.06041 uses different names for the form factors, such as $(f_0^V, f_\perp^V, f_t^V)$ instead of $(f_+, f_\perp, f_0)$, but the definitions are identical.

Dispersive bounds

The vector form factors have a branch cut starting at $t_+ = (m_B + m_K)^2$. We define the variable

$$z(t; t_0, t_+) = \frac{\sqrt{t_+ - t} - \sqrt{t_+ - t_0}}{\sqrt{t_+ - t} + \sqrt{t_+ - t_0}} \,.$$

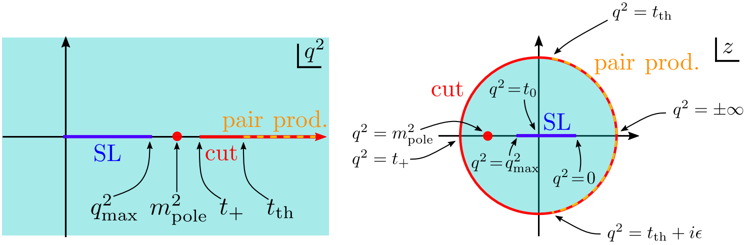

Then the dispersive bound can be written as

$$1 \geq \int_{-\alpha_{\Xi_b \Xi}}^{+\alpha_{\Xi_b \Xi}} \mathrm{d}\alpha \, \left(|\phi_{f_+}(z)|^2 |f_+(z)|^2 + |\phi_{f_\perp}(z)|^2 |f_\perp(z)|^2 \right)_{z = e^{i\alpha}}$$

where the ϕ's are the *outer functions* and

$$\alpha_{\Xi_b \Xi} = \arg z((m_{\Xi_b} + m_{\Xi})^2, t_0, t_+) \approx 1.43829 \qquad [\text{for } t_0 = q^2_{\rm max} = (m_{\Xi_b} - m_{\Xi})^2].$$

Dispersive bounds

We use BGL-type z-expansions to describe the continuum form factors,

$$f(q^2) = \frac{1}{\mathcal{P}_f(q^2)\,\phi_f(z)} \sum_n a_{f,n}\, z^n,$$

where $\mathcal{P}_f(q^2) = z(q^2; m^2_{\mathrm{pole},f}, t_+)$ is the Blaschke factor. If we had $t_{\mathrm{th}} = t_+$, so that the dispersive integral would go over the entire unit circle, we would have $1 > \sum_n (a^2_{f_+,n} + a^2_{f_\perp,n})$. Instead, because the integral only goes over a smaller arc, we have

$$1 > \sum_{n,n'} a_{f_+,n} \langle z^n | z^{n'} \rangle a_{f_+,n'} + \sum_{n,n'} a_{f_\perp,n} \langle z^n | z^{n'} \rangle a_{f_\perp,n'},$$

where [J.M. Flynn, A. Jüttner, J.T. Tsang, 2303.11285/JHEP 2023]

$$\langle z^n | z^{n'} \rangle = \begin{cases} \dfrac{\sin(\alpha_{\Xi_b\Xi}(n-n'))}{\pi(n-n')}, & n \neq n', \\[2ex] \dfrac{\pi}{\alpha_{\Xi_b\Xi}}, & n = n'. \end{cases}$$

This is equivalent to the orthogonal-polynomial expansion in [T. Blake, S. Meinel, M. Rahimi, D. van Dyk, 2205.06041/PRD 2023]

Asymptotic behavior

A possible problem with the BGL z expansion is that $\dfrac{1}{\mathcal{P}_f(q^2)\,\phi_f(z)}$ diverges for $q^2 \to -\infty$ $(z \to 1)$, while $\sum_n a_{f,n}\, z^n$ remains finite. This allows the form factor to diverge, which contradicts the expectation from perturbative QCD.

One possible solution is to use a BCL z expansion with $\dfrac{1}{1 - q^2/m^2_{\mathrm{pole},f}}$ instead of $\dfrac{1}{\mathcal{P}_f(q^2)\,\phi_f(z)}$, but then the dispersive bounds become more complicated.

We instead solve the problem by imposing the sum rules
[J.M. Flynn, A. Jüttner, J.T. Tsang, 2303.11285/JHEP 2023]

$$\left(\frac{\mathrm{d}}{\mathrm{d}z}\right)^m \sum_{n=0}^{N+M} a_{f,n} z^n \bigg|_{z=1} = 0 \qquad \forall m \in \{0, 1, ..., M-1\}$$

with $M = 4$ for f_+, g_+, $h_\perp$, and $\tilde{h}_\perp$ and $M = 3$ for the other form factors, which, given our outer functions, ensures fall-off at least as fast as $1/(-q^2)$ for $q^2 \to -\infty$. We solve for the highest M coefficients in terms of the lower coefficients.

Lattice-spacing and pion-mass dependence

We fit the lattice data using

$$
\begin{aligned}
f(q^2) \quad = \quad & \frac{1}{\mathcal{P}_f(q^2)\phi_f(q^2)}\Bigg[a_{f,0}\left(1+c_0^f\,\frac{m_\pi^2-m_{\pi,\mathrm{phys}}^2}{\Lambda_\chi^2}+\tilde{c}_0^f\,\frac{m_\pi^3-m_{\pi,\mathrm{phys}}^3}{\Lambda_\chi^3}\right)\\
&\qquad +a_{f,1}\left(1+c_1^f\,\frac{m_\pi^2-m_{\pi,\mathrm{phys}}^2}{\Lambda_\chi^2}+\tilde{c}_1^f\,\frac{m_\pi^3-m_{\pi,\mathrm{phys}}^3}{\Lambda_\chi^3}\right)z(q^2,q^2_{\mathrm{max}},t_+^f)\\
&\qquad +\sum_{n=2}^{N+M}a_{f,n}\,[z(q^2,q^2_{\mathrm{max}},t_+^f)]^n\Bigg]\\
&\times\Big[1+b^f\,a^2|\mathbf{p}'|^2+d^f\,a^2\Lambda_{\mathrm{had}}^2+\tilde{b}^f\,a^4|\mathbf{p}'|^4+\hat{d}^f\,a^3\Lambda_{\mathrm{had}}^3+\tilde{d}^f\,a^4\Lambda_{\mathrm{had}}^4+j^f\,a^4|\mathbf{p}'|^2\Lambda_{\mathrm{had}}^2\Big],
\end{aligned}
$$

where the higher-order parameters $\tilde{c}_0^f$, $\tilde{c}_1^f$, $\tilde{b}^f$, $\hat{d}^f$, $\tilde{d}^f$, and j^f, which are not needed to describe the data, were constrained with Gaussian priors to be not unnaturally large.

Statistical approach

We use the algorithm of [J.M. Flynn, A. Jüttner, J.T. Tsang, 2303.11285/JHEP 2023], which involves an initial fit with a Gaussian prior on the dispersive-bound function, followed by random sampling and an accept-reject step to apply the dispersive bound and reweight to remove the initial prior.

We increase the order of the z expansion until the central values and uncertainties of the form factors stabilize in the full kinematic range. We found that we need $N = 5$ (and recall that there are an additional $M = 3$ or $M = 4$ higher powers, so we go up to z^8 or z^9).

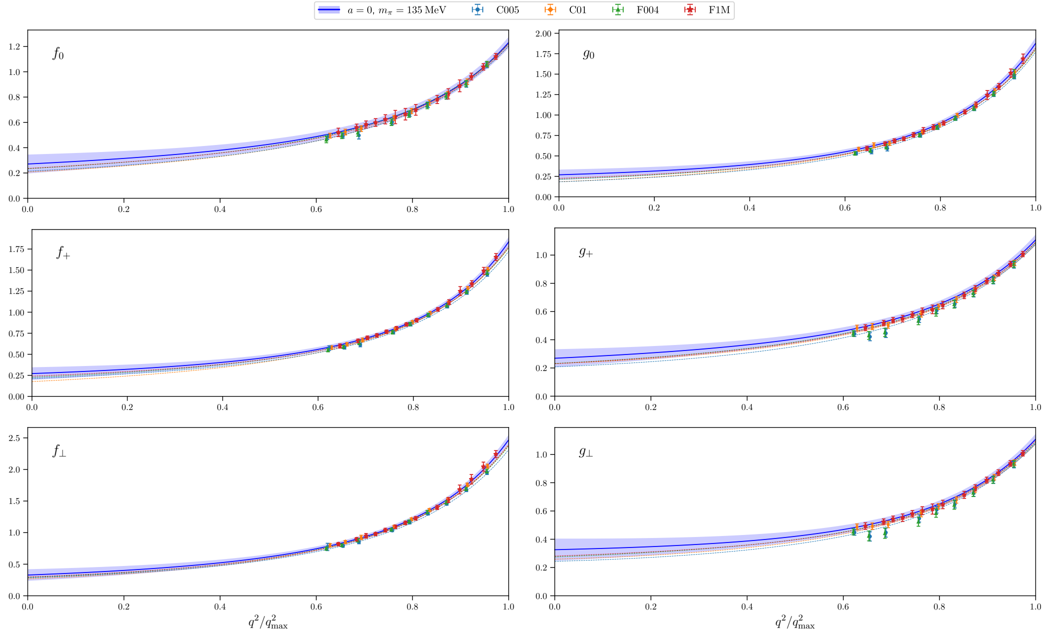

$a=0,\ m_\pi = 135$ MeV
C005
C01
F004
F1M
f_0
g_0
f_+
g_+
$f_\perp$
$g_\perp$
$q^2/q^2_{\max}$
$q^2/q^2_{\max}$

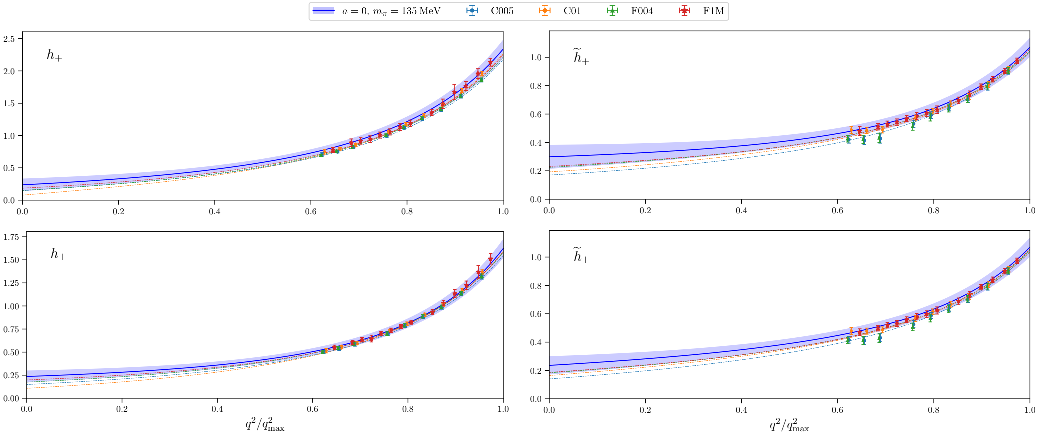

$a = 0,\ m_\pi = 135$ MeV
C005
C01
F004
F1M
h_+
$\widetilde{h}_+$
$h_\perp$
$\widetilde{h}_\perp$
$q^2/q^2_{\rm max}$
$q^2/q^2_{\rm max}$

Weak effective Hamiltonian for $b \to s\ell^+\ell^-$, $b \to s\gamma$

$$\mathcal{H}_{\text{eff}} = -\frac{4G_F}{\sqrt{2}} V_{tb} V_{ts}^* \sum_i C_i O_i$$

with

$$\begin{aligned}
O_1 &= \bar{c}^b \gamma^\mu b_L^a \;\; \bar{s}^a \gamma_\mu c_L^b, \\
O_2 &= \bar{c}^a \gamma^\mu b_L^a \;\; \bar{s}^b \gamma_\mu c_L^b, \\
O_7 &= (e\, m_b)/(16\pi^2)\;\; \bar{s} \sigma^{\mu\nu} b_R \;\; F_{\mu\nu}^{(\text{e.m.})}, \\
O_9 &= e^2/(16\pi^2)\;\; \bar{s}\gamma^\mu b_L \;\; \bar{\ell}\gamma_\mu \ell, \\
O_{10} &= e^2/(16\pi^2)\;\; \bar{s}\gamma^\mu b_L \;\; \bar{\ell}\gamma_\mu \gamma_5 \ell, \\
&\dots
\end{aligned}$$

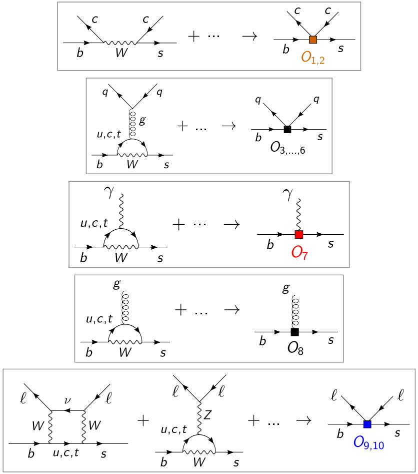

In the Standard Model, $\overline{\text{MS}}$ scheme, at $\mu = 4.2$ GeV,

C_1	C_2	C_7	C_9	C_{10}	...
−0.289	1.010	−0.336	4.267	−4.113	...

[Computed using EOS, `https://eoshep.org/`]

Hadronic matrix elements

For $\Xi_b \to \Xi \ell^+ \ell^-$ or $\Xi_b \to \Xi \gamma$:

Contributions from O_7, $[O_9,\ O_{10}]$: $\langle \Xi(p') | \, \bar{s} \Gamma b \, | \Xi_b(p) \rangle$ $\to$ local form factors

Contributions from $O_{1,\ldots,6}$, O_8: $\int \mathrm{d}^4 x \;\; e^{iq\cdot x} \langle \Xi(p') | \, \mathrm{T}\{ O_i(0) \, J^{\mu}_{\mathrm{e.m.}}(x) \} \, | \Xi_b(p) \rangle$ $\to$ nonlocal form factors

Calculation of $\Xi_b^- \to \Xi^- \mu^+ \mu^-$ and $\Xi_b^- \to \Xi^- \gamma$ observables

We treat the contributions from $O_{1,\ldots,6}$, O_8 using the OPE

$$i \sum_{i=1,\ldots,6,8} C_i \int d^4x \, e^{iq\cdot x} \, \mathrm{T}\left\{ O_i(0) \, J^\mu_{\rm e.m.}(x) \right\}$$

$$\approx \frac{1}{16\pi^2} \left[\left(q_\mu q_\rho - q^2 g_{\mu\rho} \right) \Delta C_9(q^2) \, \bar{s}\gamma^\rho b_L + 2 i m_b \, q^\rho \, \Delta C_7(q^2) \, \bar{s}\sigma_{\mu\rho} b_R \right]$$

with

$$\Delta C_7(q^2) = -\frac{1}{3}\left[C_3 + \frac{4}{3} C_4 + 20\, C_5 + \frac{80}{3} C_6 \right] - \frac{\alpha_s}{4\pi} \left[(C_1 - 6\, C_2)\, F^{(7)}_{1,c}(q^2) + C_8\, F^{(7)}_8(q^2) \right],$$

$$\begin{aligned}\Delta C_9(q^2) = {} & \frac{4}{3} C_3 + \frac{64}{9} C_5 + \frac{64}{27} C_6 + h(0,q^2)\left(-\frac{1}{2} C_3 - \frac{2}{3} C_4 - 8\, C_5 - \frac{32}{3} C_6 \right) \\ & + h(m_b,q^2)\left(-\frac{7}{2} C_3 - \frac{2}{3} C_4 - 38\, C_5 - \frac{32}{3} C_6 \right) + h(m_c,q^2)\left(\frac{4}{3} C_1 + C_2 + 6\, C_3 + 60\, C_5 \right) \\ & - \frac{\alpha_s}{4\pi}\left[C_1\, F^{(9)}_{1,c}(q^2) + C_2\, F^{(9)}_{2,c}(q^2) + C_8\, F^{(9)}_8(q^2) \right]\end{aligned}$$

[see D. Du *et al.*, 1510.02349/PRD 2016 and references therein]

$\Xi_b^- \to \Xi^- \mu^+ \mu^-$ Standard-Model predictions

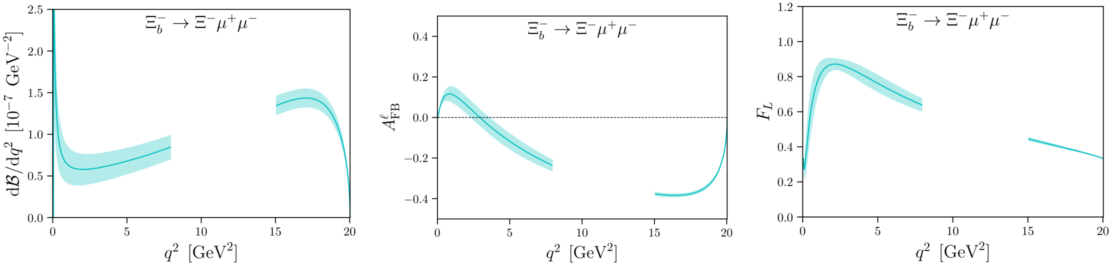

(Restricted to the kinematic regions $q^2 < 8\ \mathrm{GeV}^2$ and $q^2 > 15\ \mathrm{GeV}^2$ to avoid the effects of narrow charmonium resonances)

$\Xi_b^- \to \Xi^-\gamma$ Standard-Model predictions

	Method	$h_\perp(0) = \tilde{h}_\perp(0)$	$\mathcal{B}(\Xi_b^- \to \Xi^-\gamma)$
LHCb, 2108.07678/PRD 2022	Experiment		$< 1.3 \times 10^{-4}$
This work	Lattice QCD	0.236 ± 0.065	$(2.9 \pm 1.6) \times 10^{-5}$
Rui *et al.*, 2512.19429/PRD 2026	pQCD approach	$0.338^{+0.015+0.009+0.024}_{-0.000-0.000-0.015}$	
Aliev *et al.*, 2312.00461/PRD 2024	Light-cone sum rules	0.31 ± 0.04	$(4.8 \pm 1.3) \times 10^{-5}$
Davydov *et al.*, 2208.00833/MPL 2022	Relativistic quark model	0.144 ± 0.007	$(0.95 \pm 0.15) \times 10^{-5}$
Geng *et al.*, 2202.06179/PRD 2022	Light-front quark model	0.143	$(1.1 \pm 0.1) \times 10^{-5}$
Olamaei *et al.*, 2109.09783/EPJC 2022	Light-cone sum rules		$(1.08^{+0.63}_{-0.49}) \times 10^{-5}$
Wang *et al.*, 2008.06624/JPG 2021	Flavor-$SU(3)$ symmetry		$(1.23 \pm 0.64) \times 10^{-5}$
Liu *et al.*, 1103.0081/PRD 2011	Light-cone sum rules	≈ 0.6	$(3.03 \pm 0.10) \times 10^{-4}$

Outlook: next-generation $\Lambda_b \to p, \Lambda, \Lambda_c$ form-factor calculations

Goals of the next-generation calculations:

- Higher precision
- Controlled uncertainties in full kinematic range
- Satisfy FLAG quality criteria

Parameters of the 2015/2016 calculations

Label	$N_s^3 \times N_t$	β	$am_{u,d}^{(\mathrm{sea})}$	$am_{u,d}^{(\mathrm{val})}$	$am_s^{(\mathrm{sea})}$	$am_s^{(\mathrm{val})}$	a [fm]	$m_\pi^{(\mathrm{sea})}$ [MeV]	$m_\pi^{(\mathrm{val})}$ [MeV]	Samples
C14	$24^3 \times 64$	2.13	0.005	0.001	0.04	0.04	≈ 0.111	≈ 340	≈ 250	2672
C24	$24^3 \times 64$	2.13	0.005	0.002	0.04	0.04	≈ 0.111	≈ 340	≈ 270	2676
C54	$24^3 \times 64$	2.13	0.005	0.005	0.04	0.04	≈ 0.111	≈ 340	≈ 340	2782
C53	$24^3 \times 64$	2.13	0.005	0.005	0.04	0.03	≈ 0.111	≈ 340	≈ 340	1205
F23	$32^3 \times 64$	2.25	0.004	0.002	0.03	0.03	≈ 0.083	≈ 304	≈ 230	1907
F43	$32^3 \times 64$	2.25	0.004	0.004	0.03	0.03	≈ 0.083	≈ 304	≈ 304	1917
F63	$32^3 \times 64$	2.25	0.006	0.006	0.03	0.03	≈ 0.083	≈ 361	≈ 361	2782

These data sets come from three ensembles only. The red color indicates $m_{u,d}^{(\mathrm{val})} < m_{u,d}^{(\mathrm{sea})}$, leading to small $m_\pi^{(\mathrm{val})} L$ and making finite-volume errors the dominant systematic uncertainty.

The bottom-quark parameters violate the kinetic-mass tuning condition by $O(10\%)$
[S. Meinel, 2309.01821/PoS 2024]

The extrapolations to $q^2 = 0$ use first-order z expansions only, with ad-hoc estimates of missing higher-order terms.

Parameters of the next-generation calculations

Label	$N_s^3 \times N_t$	β	$am_{u,d}^{(\mathrm{sea,val})}$	$am_s^{(\mathrm{sea})}$	$am_s^{(\mathrm{val})}$	a [fm]	$m_\pi^{(\mathrm{sea,val})}$ [MeV]	Samples
CP	$48^3 \times 96$	2.13	0.00078	0.0362	0.0362	≈ 0.114	≈ 139	80 ex, 2560 sl
CPB*	$48^3 \times 96$	2.13	0.00078	0.0362	0.0362	≈ 0.114	≈ 139	78 ex, 2496 sl
C005LV	$32^3 \times 64$	2.13	0.005	0.04	0.0323	≈ 0.111	≈ 340	186 ex, 5022 sl
C005	$24^3 \times 64$	2.13	0.005	0.04	0.0323	≈ 0.111	≈ 340	311 ex, 4976 sl
F004	$32^3 \times 64$	2.25	0.004	0.03	0.0248	≈ 0.083	≈ 304	251 ex, 4016 sl
F006	$32^3 \times 64$	2.25	0.006	0.03	0.0248	≈ 0.083	≈ 361	223 ex, 3568 sl
F1M	$48^3 \times 96$	2.31	0.002144	0.02144	0.02217	≈ 0.073	≈ 232	226 ex, 7232 sl

*same ensemble, but half the source/sink smearing width for propagators; different subset of configs

Six different ensembles, all data sets use $m_{u,d}^{(\mathrm{val})} = m_{u,d}^{(\mathrm{sea})}$. Now using physical $am_s^{(\mathrm{val})}$.

I have newly computed all propagators with improved source smearing, and using all-mode averaging [E. Shintani *et al.*, 1402.0244/PRD 2015].

I have re-tuned the bottom and charm action parameters [S. Meinel, 2309.01821/PoS 2024].

Simultaneous fits of CP and CPB data $\Lambda_b \to \Lambda_c$

preliminary

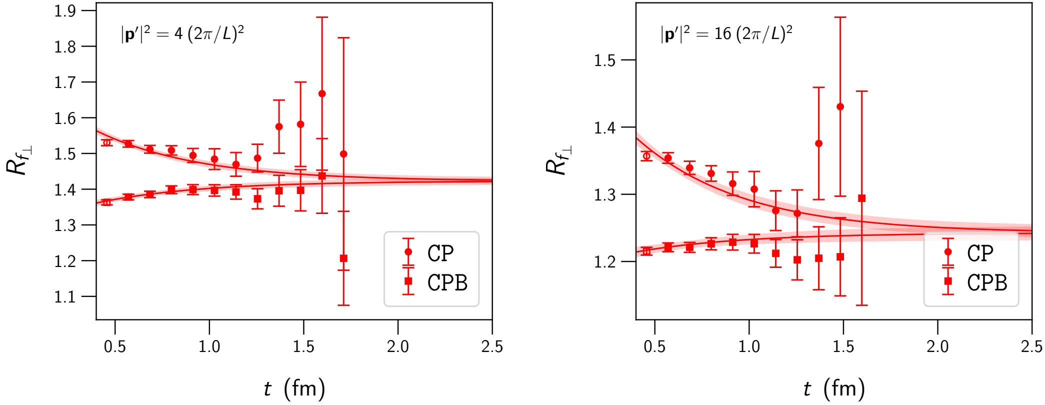

Simultaneous fits of CP and CPB data $\Lambda_b \to \Lambda$

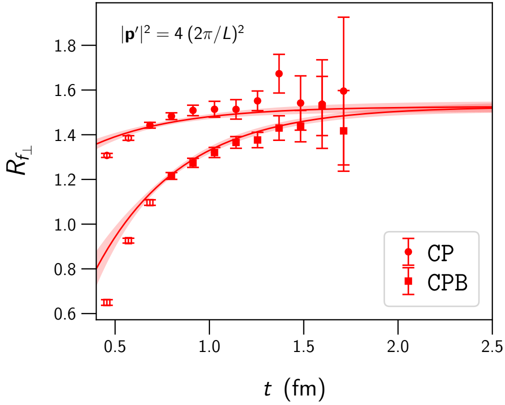

preliminary

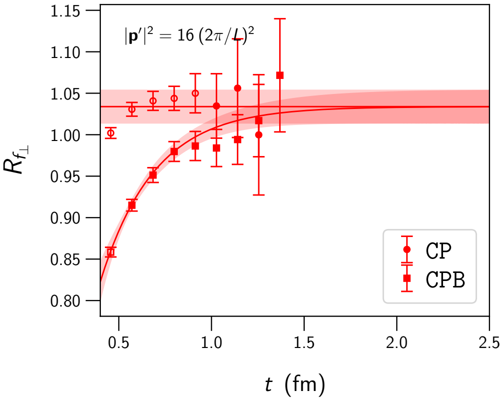

Simultaneous fits of CP and CPB data

$\Lambda_b \to p$

preliminary

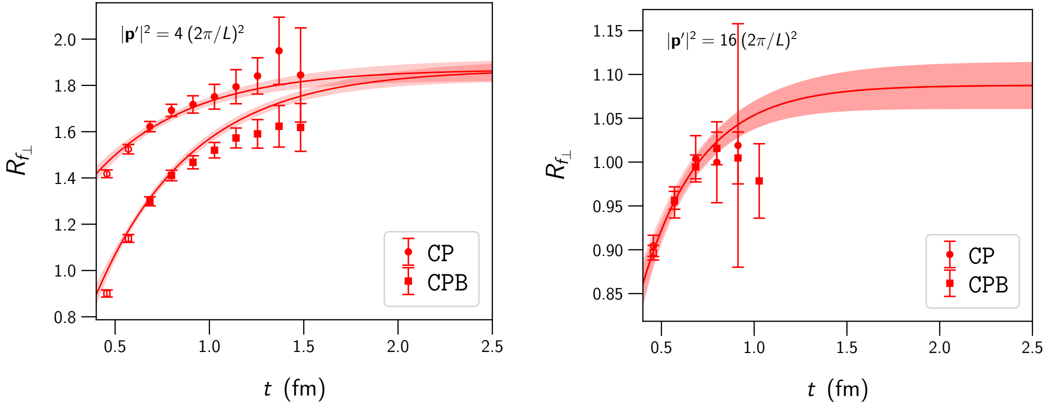

Preliminary chiral-continuum-kinematic extrapolations

Some systematic uncertainties not yet included.

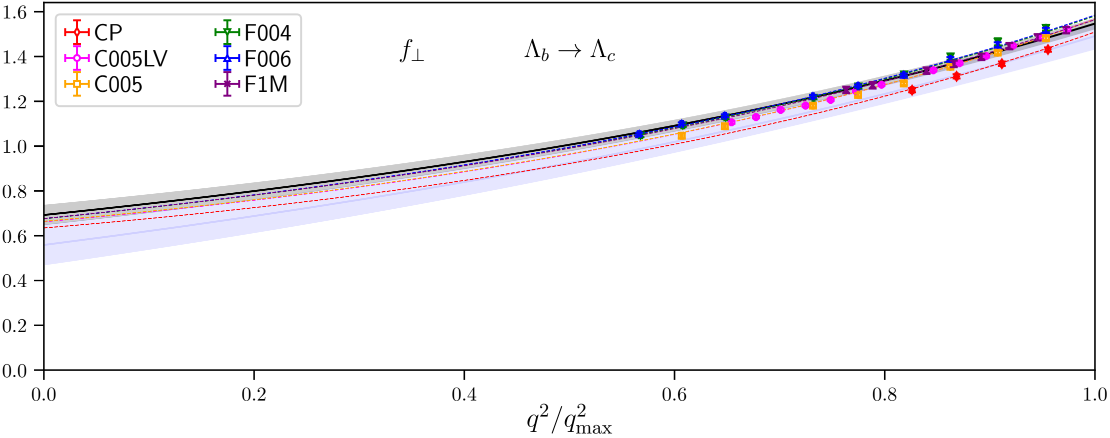

Black curve = preliminary new continuum form factor (fit with $N = 5$ and dispersive bound).
Light-blue curve = 2015 form factor

Preliminary chiral-continuum-kinematic extrapolations

Some systematic uncertainties not yet included.

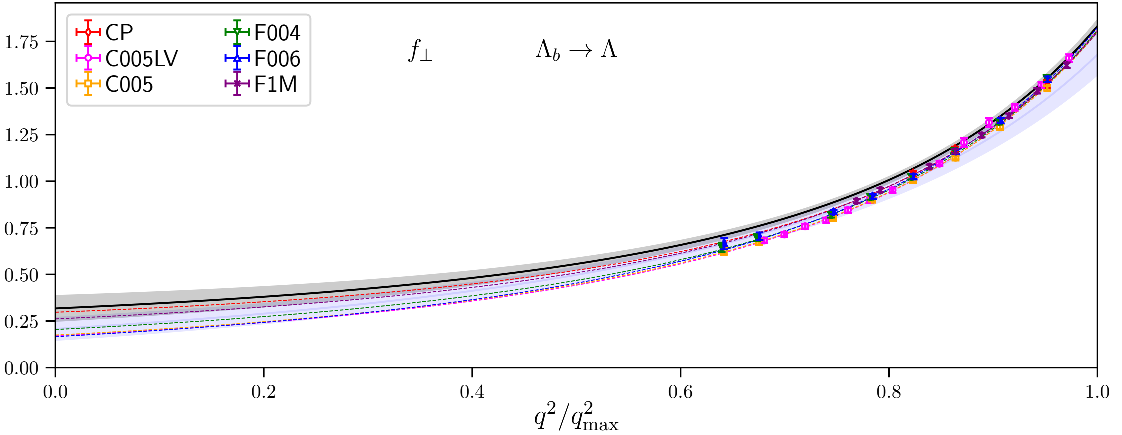

Black curve = preliminary new continuum form factor (fit with $N = 5$ and dispersive bound).
Light-blue curve = 2016 form factor

Preliminary chiral-continuum-kinematic extrapolations

Some systematic uncertainties not yet included.

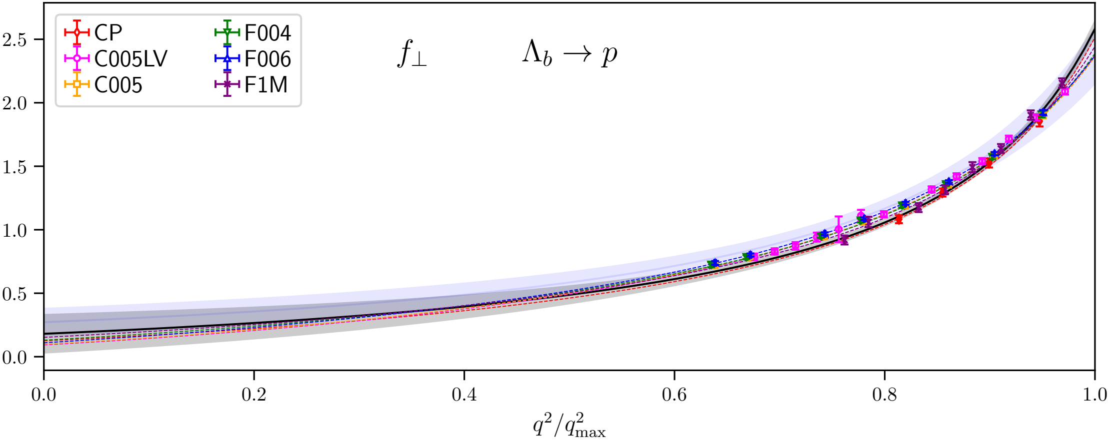

Black curve = preliminary new continuum form factor (fit with $N = 5$ and dispersive bound).
Light-blue curve = 2015 form factor

Funding acknowledgment: This work was supported by the U.S. Department of Energy, Office of Science, Office of High Energy Physics under Award Number DE-SC0009913.